



## Seismic Site Characterization at Strong Motion Stations in Metro Vancouver

Jamal Assaf<sup>1</sup>, Sheri Molnar<sup>2</sup>, Hesham El Naggar<sup>3</sup>, Aamna Sirohey<sup>4</sup>

<sup>1</sup> Ph.D. Candidate, Department of Civil and Building Engineering, Western University - London, ON, Canada.

<sup>2</sup> Assistant Professor, Department Earth Science, Western University - London, ON, Canada.

<sup>3</sup> Professor, Department of Civil and Environmental Engineering, Western University - London, ON, Canada.

<sup>4</sup> MSc. Student, Department Earth Science, Western University - London, ON, Canada.

### ABSTRACT

The present free-field strong motion network in Vancouver has recorded several moderate earthquakes since 2002. Meanwhile, there is no detailed understanding of the seismic properties of the soil deposits at these stations. Proper site characterization at these sites should help in correlating the observed ground motions with the underlying soil properties and understanding the regional site effect hazard in the region. Non-invasive methods using surface wave techniques have been proven to be cost effective and reliable methods to characterize the seismic properties at a specific site. Combined active-source Multichannel Analysis of Surface Waves (MASW) and passive-source Microtremor Array Method (MAM) measurements were performed in July 2018 and co-located with 20 strong motion stations in Metro Vancouver to develop shear wave velocity ( $V_s$ ) profiles. This testing campaign is part of a multi-year seismic microzonation project aimed at identifying local variations of site response across western Metro Vancouver. The fundamental-mode Rayleigh wave dispersion curve and microtremor horizontal-to-vertical spectral ratio are extracted from the non-invasive seismic measurements at each site. This paper outlines how joint inversion of the experimental data is performed and presents preliminary  $V_s$  profiles for 4 sites. The  $V_s$  profiles will be used to refine the current earthquake site classification map of Metro Vancouver as well as to calculate theoretical 1D site amplification for validation with empirical site amplification in southwest British Columbia.

Keywords: seismic hazard, site effects, microzonation, site characterization, site assessment, non-invasive methods,  $V_s$ .

### INTRODUCTION

British Columbia (BC), is located in one of the most seismically active regions in Canada. Southwestern BC, including Metropolitan (Metro) Vancouver, has the highest seismic risk in Canada due to the complex geologic and tectonic setting of the region [1]. The alluvial sediments in Fraser River Delta, south Vancouver, are known to significantly modify the amplitude and frequency of seismic waves [2]. Amplification hazard in Vancouver has mainly been associated with the presence of these deep soft soils in the Delta. Thus, an accurate estimation of local geology effect on earthquake ground motion is critical for seismic hazard assessment to ensure the safety of communities in that area. The strong motion station network in Metro Vancouver has recorded more than 7 earthquake events since 1976. However, the lack of detailed characterization of the soils at the locations of these stations does not allow for a proper correlation between the observed ground motions and the local geology.

Local site effect, or earthquake site response, is the effect of near surface geology on the propagation of seismic waves in the upper few hundred meters [3]. The variation of stiffness, described by shear wave velocity ( $V_s$ ), and geometry of the soil at the site of interest can modify the amplitude and frequency of seismic waves. Borcherdt [4] proposed  $V_{S30}$ , the time averaged  $V_s$  in the top 30 m, as a parameter to quantify seismic site classes and their potential to amplify ground motions. Since then,  $V_{S30}$  has been incorporated in many building codes around the world to account for site effects. However, many studies on observed earthquake ground motions showed that  $V_{S30}$ , restricted to the top 30 m, is unable to fully capture site effects, especially at deep sites or when strong impedance contrasts are present [5]. Alternatively, theoretical site response can be computed and compared to observed site response when site conditions at the earthquake recording site are well known, which is rarely the case. Hence, determining subsurface site conditions, i.e.,  $V_s$  depth profile(s), at Vancouver strong motion stations is required to calculate theoretical site response predictions for validation with the observed site response.

Time efficiency and cost effectiveness have been always considered in choosing adequate  $V_s$  profiling methods. In engineering practice, borehole invasive methods such as seismic cross-hole, seismic downhole and PS suspension logging are usually used to determine localized  $V_s$  profiles with high resolution. These methods may be expensive and time consuming when drilling to significant depths is needed or when stiff, interbedded soil deposits exist [6]. Recently, cost-effective noninvasive surface

wave techniques have become very popular to infer reliable  $V_s$  profiles with similar uncertainty compared to invasive borehole methods [9,10]. These techniques measure surface wave dispersion at the site of interest which is inverted to find  $V_s$  profile(s) in agreement with the experimental dispersion data.

Surface wave techniques usually involve three phases: (1) acquisition of data, (2) dispersion analysis, and (3) inversion [9]. In the first phase, active- and/or passive-source vibrations are measured using single or three component sensors. Active-source vibrations generated by artificial sources, such as explosives, sledge hammer or weight drop, are rich in high frequencies, whereas passive-source vibrations are generated by natural phenomena at low frequencies ( $< 1$  Hz) and anthropogenic sources at higher frequencies ( $> 1$  Hz) [10]. Due to the difference in the nature of their source wave field, active- and passive-source surface wave measurements allow the characterization of shallow and deep sediments, respectively. The combination of the two methods is often recommended to obtain the dispersion curve over a wide frequency (wavelength) range.

Inversion of the site's dispersion curve aims at finding a layered earth model whose theoretical (forward) dispersion curve "best" fits the experimental one. The best-fit model is often defined as having the minimum misfit with the experimental data. Joint inversion of dispersion estimates with an amplification curve (measured from microtremor horizontal to vertical spectral ratios, MHVSR) is often accomplished. Sole inversion of either dispersion or MHVSR amplification response are inherently non-linear and non-unique. Joint inversion of both datasets together aids in constraining  $V_s$  depth profiles that adequately fit both datasets. Dispersion estimates are typically defined at higher frequencies and constrain near-surface model velocities, whereas MHVSRs constrain model velocities at depth because MHVSRs exhibit amplification at peak frequencies related to significant impedance contrasts at depth (the fundamental peak frequency is related to depth to resonator or seismic bedrock, i.e., total soil thickness). Additional known *a priori* information on the geologic stratigraphy of the test area can greatly help in constraining the inversion process and preventing it from resulting in unrealistic  $V_s$  models.

This paper describes combined active- and passive-source surface wave array measurements conducted near 20 strong-motion station locations as part of an ongoing microzonation-mapping project for Metro Vancouver. Details of active- and passive-source surface wave array measurement and dispersion analyses are presented here. Results of preliminary joint inversion of the dispersion curves and MHVSRs at 4 sites are presented. Obtaining  $V_s$  profiles at all strong motion station sites will allow for a thorough comparison between observed and 1D theoretical site response in Vancouver.

## LOCATION AND TESTING METHODS

The Fraser River (FR) delta, south of Vancouver city, is made up of soft Holocene sediments mainly silts and sands up to 300 m thickness that have been deposited since the last glaciation 11,000 years ago [11]. These Holocene deltaic sediments overlie Pleistocene sediments mostly composed of ice-compacted till and glaciomarine silts and sands. This Holocene-Pleistocene sediment package overlies Tertiary sedimentary bedrock and pinches out to the north from a maximum thicknesses of about 800 m in Ladner to only several meters at the edge of the delta [12]. Tertiary bedrock outcrops in Queen Elizabeth Park in Vancouver and in Stanley Park sea cliffs. Tertiary bedrock dips to the south and consists of Miocene sandstone and shales reaching 200 m to 1000 m depth underneath the FR delta [12]. The shear wave velocity measurements in the Holocene FR delta have an average  $V_s$  of 200 - 300 m/s, starting with  $\sim 71$  m/s near surface and increasing with depth [13]. The average velocity of Pleistocene glacial sediments is  $\sim 500$  m/s and the Tertiary bedrock velocity is more than 1500 m/s [14]. The 4 selected sites in this study are shown in Figure 1a, in comparison to the current seismic site class map for Metro Vancouver based on geologic units and their average velocities measured in the Lower Mainland [15].

The four selected surface wave array testing sites, RI091, RI095, VA051 and VA072, are within 430 m distance of strong motions, RMD02, RMD01, VNC23 and VNC22, respectively [16]. Array site RI091 is located near the north arm of the Fraser River where Pleistocene sediments are found at a depth of about 50 m below the surface [14]. This depth increases to the south beneath array site RI095 where soft, deltaic sediments become thicker [13]. The 2 Vancouver array sites, VA051 and VA072, are about 4 km north of the Fraser River's northern arm where stiff Pleistocene sediments are present.

During a one-month field campaign in July 2018, active- and passive-source array measurements were conducted at 44 sites in Metro Vancouver. The locations of these measurements were chosen in efforts to characterize the subsurface conditions near strong motion stations and to provide adequate spatial coverage across Metro Vancouver. Hence, 20 of these 44 array sites are within a distance of 430 m from strong motion stations.

Passive MAM measurements were recorded using 3-component velocimeter sensors (Tromino<sup>®</sup>), deployed in a circular array geometry with a central sensor (Figure 1b). The sensors were installed in 4 different sized arrays with varying radial distances of 5, 10, 15 and 30 m. Ambient vibrations were recorded simultaneously by all sensors with 30 minute duration for the largest array (30 m) and at least 15 minute duration for each smaller array. At some sites, the largest array could not be achieved due to spatial constraints, and thus a smaller spacing was used. For example, largest array radial distance is 25 m at site VA072. Varying the array aperture allows the extraction of dispersion curves over a wide range of frequencies where smaller arrays provide reliable velocity estimates at higher frequencies and larger arrays provide reliable estimates at lower frequencies.

Active MASW measurements were conducted using 24 vertical-component 4.5-Hz geophones deployed in a linear array. Receiver spacings were set to 0.5, 1 and 3 m. A 5 kg hammer was used to generate the pulse wave with a 5 m source offset to

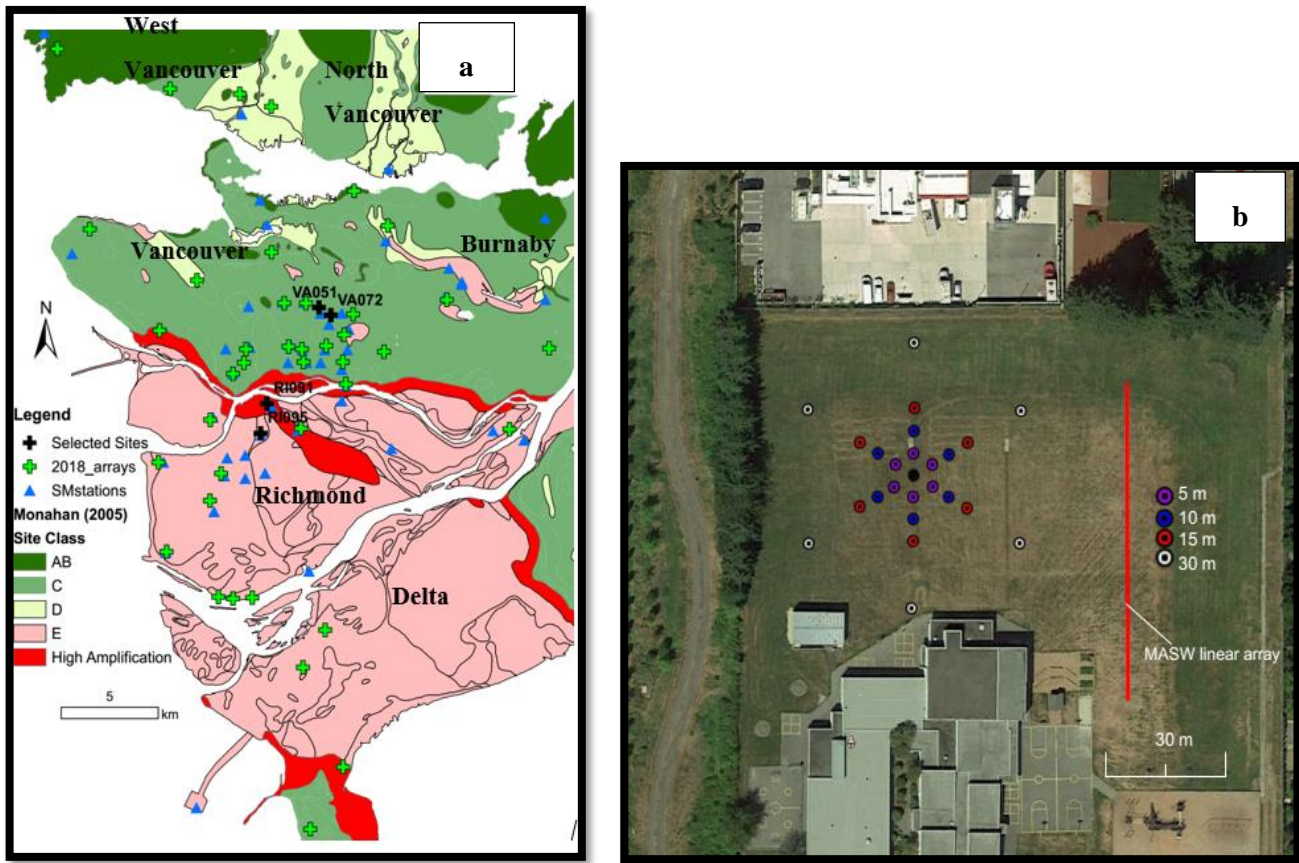


Fig. 1a: Location of array measurements conducted in July 2018 (green crosses) and co-located with strong motion stations (blue triangles) in Metro Vancouver. Site Class microzonation map is modified from [15]. 1b: Geometry of passive circular arrays and MASW linear array location at Site RI095.

the first geophone for 0.5 and 1 m spacings and 10 m offset for 3 m spacing. MASW array testing was conducted at most sites where space was available. For 0.5 and 1 m spacings, several forward and backward shots were recorded, while, forward, backward, and middle shots were recorded for 3 m spacing.

## PROCESSING

The active- and passive-source raw array recordings were processed using the open source Geopsy software (v. 2.9.1, [17]). The MHVSR curves were calculated for each sensor location in the passive-source circular array. Time series quality and synchronization between the three components were checked before dividing each record into 60 s time windows; this length was chosen to ensure low frequency data is well retrieved. The time windows were then converted into frequency domain and smoothed using a Konno and Omachi [18] technique with a bandwidth of 40. The squared-average horizontal components spectrum was divided by the vertical spectrum to obtain MHVSR curves for each time window and the average of all windows was calculated. Time windows showing erroneous (inconsistent) MHVSR spectrum were disregarded. The MHVSR curves from all sensors of the 5-m smallest and 30-m largest array apertures were compared to verify consistency in MHVSR response and the lateral homogeneity assumption at the sites. Finally, the spatial average MHVSR curve computed from the smallest and largest array sensors was selected to be used in inversion process for each site.

Dispersion analysis from the vertical-component passive-source array recordings was performed using the Modified Spatial Auto Correlation (MSPAC) method [19]. This method converts the azimuthal average of the spatial autocorrelation function derived from all time windows and spacings into dispersion estimates represented by plots of phase velocity at each selected frequency. The phase velocities calculated using all 4 array configurations were stacked together and a single fundamental-mode Rayleigh-wave dispersion curve was picked between the resolution and aliasing limits. These limits are based on the 2

frequencies at which the largest ring's autocorrelation function attains a maximum and the smallest ring's autocorrelation function attains a minimum, respectively [10].

For MASW data, the vertical component recordings containing the waveforms of hammer shots were processed using the frequency wavenumber (FK) technique [20]. Waveform amplitudes were normalized by distance to account for amplitude decay. Dispersion estimates from different shot offsets and receiver spacings were stacked and the fundamental-mode Rayleigh-wave dispersion curve was picked for inversion analysis.

## DISPERSION ANALYSIS AND PRELIMINARY SITE CLASSIFICATION

The experimental dispersion curves from active- and passive-source array recordings and MHVSR curves for the 4 selected sites are presented in Figure 2. The dispersion curves of the 2 Richmond sites are comparable where low phase velocities (< 100 m/s) at very high frequencies or very shallow depths are representative of soft sediments in FR delta area. For Vancouver sites, phase velocities of about 300 m/s are observed at high frequencies representing stiffer materials. The Holocene-Pleistocene impedance contrast underneath site RI095 can be inferred as deeper than underneath site RI091 as confirmed by the 2<sup>nd</sup> peak frequency in the MHVSR curves of both sites (0.73 Hz compared to 1 Hz, respectively) and the shift to lower frequency at which a significant increase in phase velocities estimates are obtained. The 'curvature' of the dispersion estimates is mearing the transition to higher velocity material (i.e., impedance contrast). Similar trends are observed in the dispersion and MHVSR curves in Vancouver, where the impedance contrast underneath site VA072 is deeper than that underneath VA051.

The following simplified equation [21] uses phase velocities corresponding to a 40-m wavelength Rayleigh wave,  $V_{R[40]}$ , to calculate  $V_{S30}$  within 10 % error, where

$$V_{S30} = 1.045 V_{R[40]}.$$

Using this equation, the picked dispersion estimates at RI091 and RI095 predict  $V_{S30}$  values of 198 and 200 m/s, respectively, corresponding to NBCC site class D. Vancouver sites, VA051 and VA072, correspond to site class D/C with  $V_{S30}$  values of 355 and 359 m/s, respectively. The current site class map (modified from [15]) indicates site classes E for RI095 and class C for VA051 and VA072, while RI091 is assigned as a high amplification zone based on recorded previous earthquakes where maximum ground motions were observed near the edge of the FR delta [2].

## JOINT INVERSION

Joint inversion is the process of inverting both dispersion and MHVSR curves simultaneously. Dispersion curves, obtained from active- and passive-sources, allow the estimation of shallower velocities while amplitude and frequency of MHVSR peaks constrains the impedance contrasts' velocities and depths. The dispersion phase velocity estimates were retrievable to frequencies higher than MHVSR peak frequencies. At a MHVSR peak, the vertical component amplitudes are reduced and measurement of the autocorrelation function or dispersion from the vertical component is nearly impossible. The maximum resolved wavelength ( $\lambda_{max}$ ) for each site was calculated from the experimental phase velocity at the lowest defined frequency. This parameter is conventionally used to determine the maximum resolved depth of the array ( $d_{max}$ ) where  $d_{max}$  is taken as a value between  $\lambda_{max}/3$  and  $\lambda_{max}/2$  ( $\lambda_{max}/2$  is used here) [9]. It is not recommended to allow the inverted  $V_s$  profiles to extend below this depth when only dispersion curves are inverted; nonetheless,  $V_s$  profiles here were extended deeper as MHVSR curves provides longer wavelength (deeper) data. However, it should be noted that  $V_s$  profiles past this depth are far less reliable as no phase velocity estimates are available.

The two MHVSR peaks of the Richmond sites are assumed to be representative of the impedance contrasts at the Holocene-Pleistocene and Pleistocene-bedrock interfaces, while the MHVSR peak of the Vancouver sites is presumably due to the latter. All picked MHVSR peaks satisfy SESAME guidelines (2004) clarity criteria. While several opinions exist about what parts of the MHVSR curve should be included in the joint inversion, only MHVSR peaks were used here as they are believed to be representative of subsurface site conditions. As in, the seismic wavefield that gives rise to the MHVSR functional form is still debated, whereas MHVSR peaks are known to relate to seismic impedance contrasts. Inversion of the dispersion curve alone is accomplished for comparison.

All inversions were conducted using Dinver software of the Geopsy software package. Dinver uses a global neighborhood algorithm to find theoretical ground profiles parameters whose forward solutions best fit the experimental dispersion curve and MHVSR [17]. The joint misfit function is calculated based on weights assigned to dispersion curve and Rayleigh wave ellipticity (MHVSR) misfits; equal weights were used in this study.

The required parameters for inversion are the density ( $\rho$ ), Poisson's ratio ( $\nu$ ), compressional wave velocity ( $V_p$ ),  $V_s$  and thickness ( $H$ ) of each predefined layer. The theoretical dispersion and ellipticity functions are most sensitive to  $V_s$  and  $H$  and less influenced by other parameters.  $V_p$  and Poisson's ratio were linked to  $V_s$  values in our inversion and reasonable density

estimates of the geologic units were selected and fixed in the inversion [22]. Layer velocities were assumed to increase with depth; there is no observed low velocity zones in the dispersion data. In inversion, the number of layers controls the number

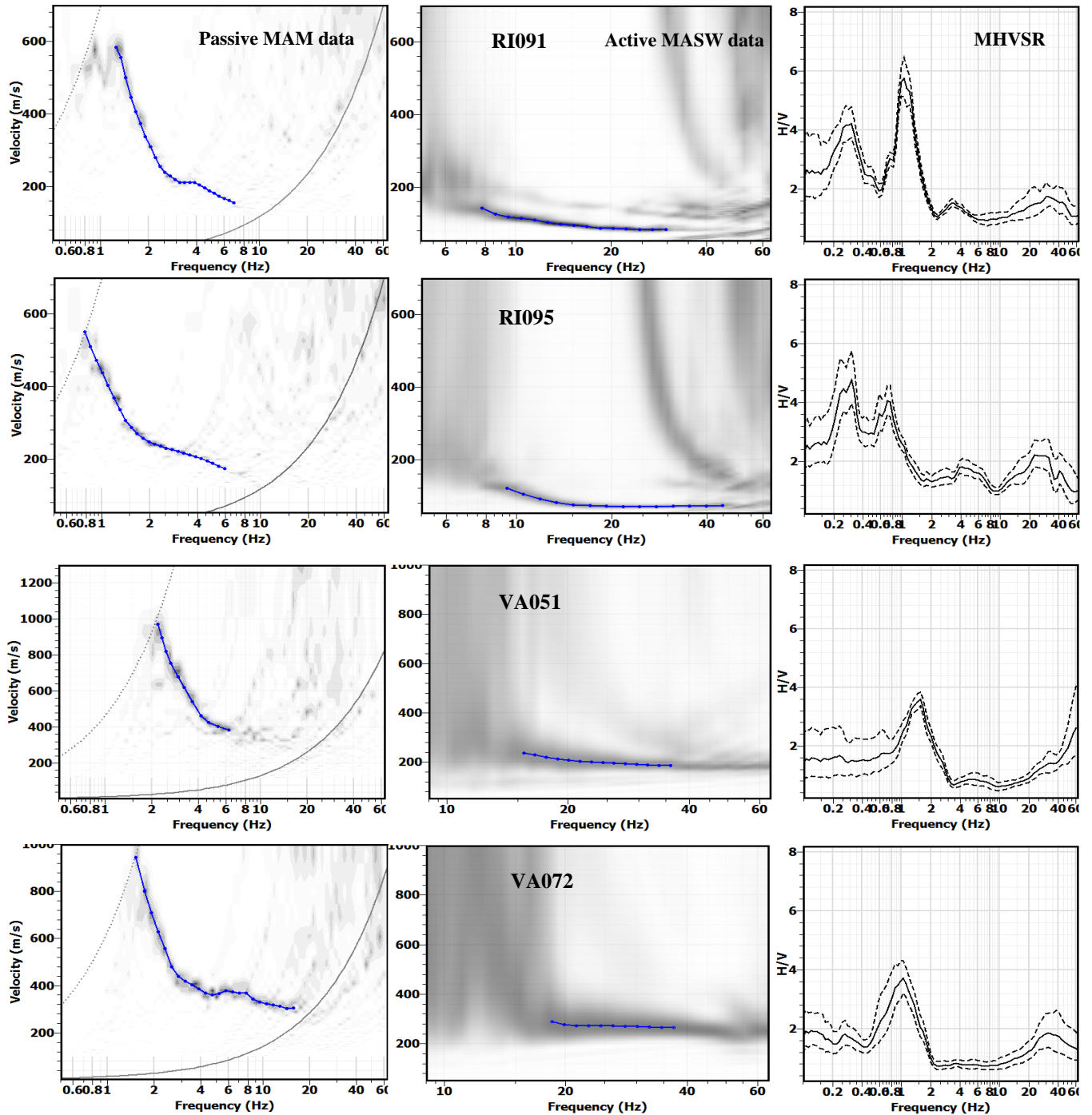


Fig. 2 Input parameters for inversion at the 4 considered sites. (Left) Dispersion estimates from passive-source MAM data with picked dispersion curve in blue. (Middle) Dispersion estimates from active-source MASW data with picked dispersion curve in blue. (Right) Average  $\pm$  one standard deviation MHVSR curve from all sensors in the smallest and largest arrays.

of unknown parameters to be solved for; however, this number of layers itself is unknown. We therefore define a single uniform layer over a homogeneous half-space model and additional layers (more parameters) are progressively added until a reasonable misfit with the experimental data is reached. Adding more layers will generally decrease the minimum misfit if enough models are searched; however, this might over parametrize the problem by adding unnecessary degrees of freedom leading to superfluous geologic complexity. For each of the layered models, a minimum of 500,000 model solutions were searched. Minimum misfit models from different model parameterizations are presented here to address some of the inversion non-

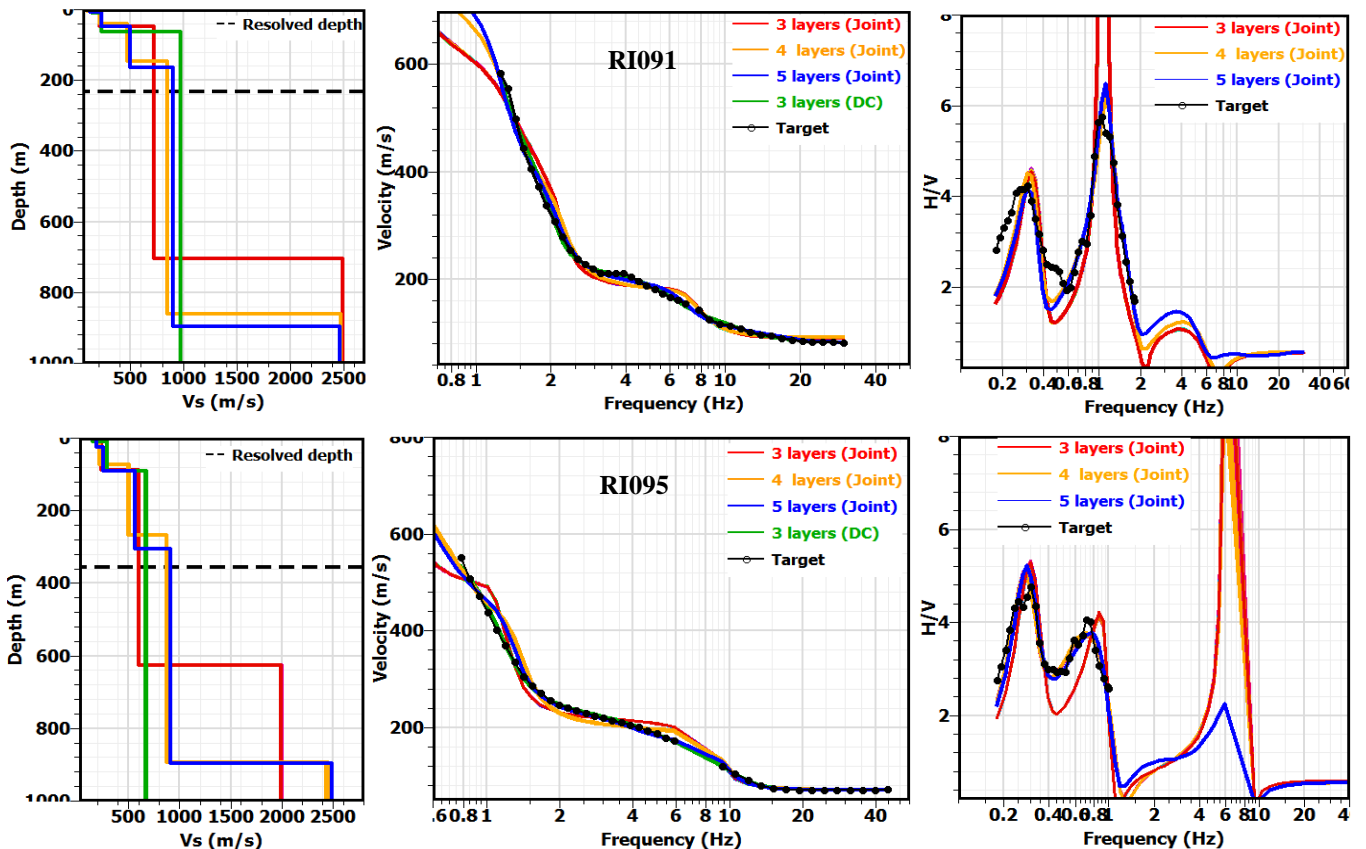
uniqueness and parametrization effect on the resulting  $V_s$  profiles. The elastic-half space was constrained to 900 m depth with a maximum  $V_s$  value of 2500 m/s. It should be noted that no geologic or depth constraints were used to guide the inversion. The final layers in the retrieved models range from 3 to 5 layers for Richmond sites and 2 to 3 layers for Vancouver sites, excluding the elastic half-space.

### $V_s$ PROFILES AND SITE CLASSIFICATION

Figure 3 presents the minimum misfit  $V_s$  profiles for the 4 sites from different model parameterizations in comparison to their forward modelled dispersion and ellipticity curves. These theoretical curves are plotted with the experimental dispersion and MHVSR data (input or targets).  $V_s$  profiles obtained from 4- and 5-layer models for Richmond sites and 2- and 3-layers for Vancouver sites show less variability amongst each other. The models' theoretical Rayleigh ellipticity fits the MHVSR peak at Vancouver sites as well as the 2<sup>nd</sup> peak at Richmond sites very well, in terms of peak frequency. The maximum assumed half-space depth (900 m) and  $V_s$  (2500 m/s) did not allow precise fitting of the low frequency peak at RI091 and RI095 sites. While  $V_s$  profiles obtained from joint inversion predict deeper impedance contrasts compared to  $V_s$  profiles obtained from dispersion inversion alone, both  $V_s$  profiles demonstrate velocity transitions at similar depths. In general,  $V_s$  variability between different minimum misfit models increases with depth. Beyond the maximum resolved depth, the  $V_s$  models are far less reliable as they are solely constrained by MHVSR peaks.

The model profiles reach  $V_s$  of 500 m/s at depths between 40 and 63 m for RI091 and between 75 and 90 m for RI095, inferred as the depth to stiff Pleistocene material. This conforms to the geological evidence indicating Holocene FR deltaic sediments thickness of ~50 m near RI091 and ~100 m at RI095 [14], even though no constraints were used during inversion. Taking into account the similarities between near surface velocities in the dispersion curves of the two sites, the 2<sup>nd</sup> peak frequencies at 1 Hz for RI091 and 0.73 Hz for RI095 may be used as a robust indicator of the thickness of the Holocene sediments. The estimated depth of the Pleistocene-bedrock interface varies between different model parameterizations for Richmond sites as it is poorly constrained by MHVSR peaks.

The resolved depths of the dispersion data for Vancouver sites are much deeper than the plotted y-axis depth limits in Figure 3. The nearest available borehole log at ~3 km to the east of Vancouver sites determines a Pleistocene-bedrock interface at a depth of 115 m [23]. The predicted half-space depth (inferred bedrock) at stiffer Vancouver sites reasonably ranges between 57 and 70 m depth at VA051 and between 77 and 93 m depth at VA072. The joint inversion predicts a deeper interface than the inversion of the dispersion curve alone as additional constraint on the peak frequency is applied in the inversion.



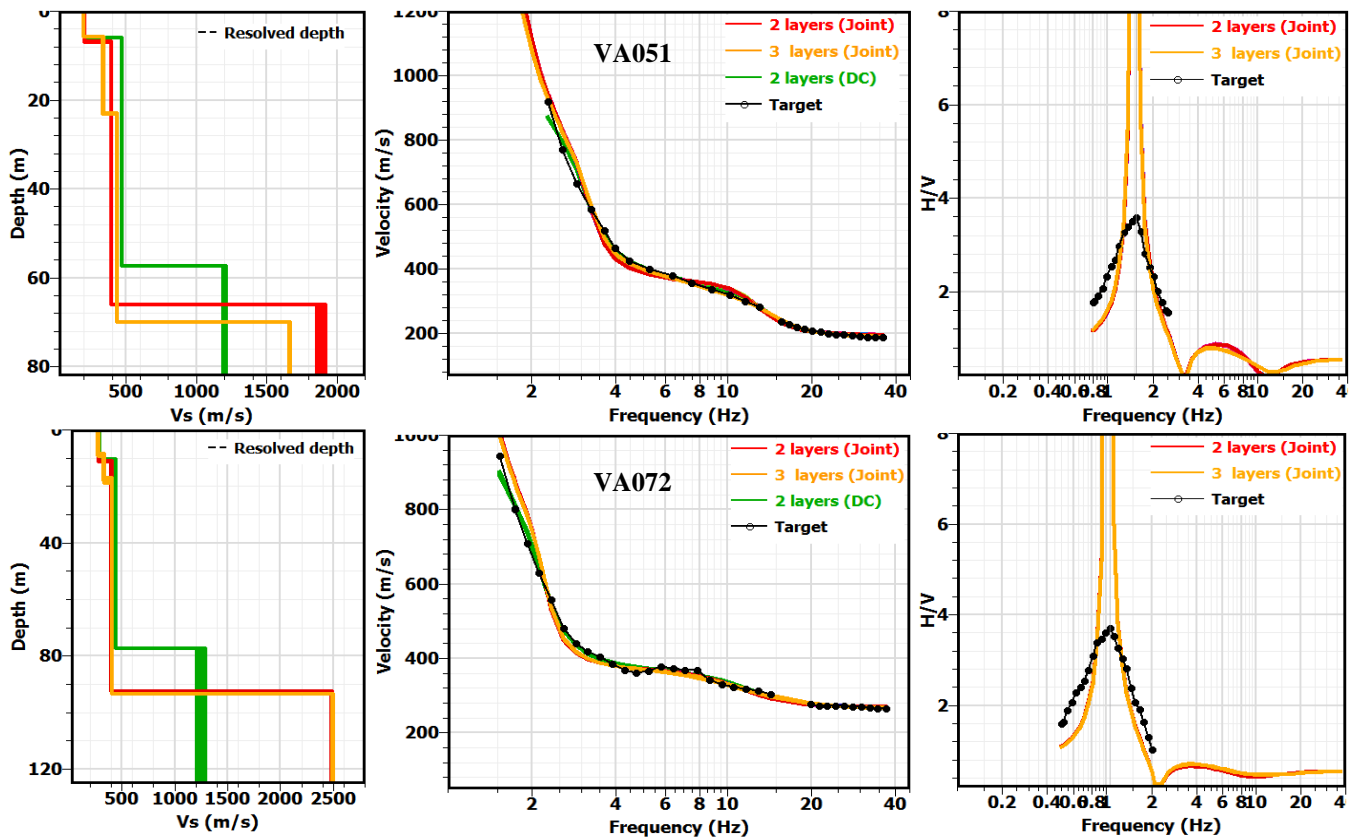


Figure 3: Shear wave velocity profiles obtained with different model parameterizations for the 4 selected sites (left), the theoretical and experimental phase velocity dispersion curves (middle), and theoretical ellipticity function with experimental MHVSR peaks (left). Joint refers to joint inversion results and DC refers to dispersion inversion only.

At the moment, there are no available borehole logs in the immediate vicinity of these Vancouver sites for validation of the inverted  $V_s$  profile.

## CONCLUSIONS AND RECOMMENDATIONS

This paper describes the non-invasive surface wave measurements campaign, conducted in July 2018, to characterize the seismic shear wave velocities at 20 strong motion stations as a part of an ongoing seismic microzonation project of Metro Vancouver. Both active-source MASW and passive-source MAM techniques were implemented to measure surface wave dispersion at the sites; 4 selected sites are presented in this paper. Dispersion and MHVSR curves obtained from processing MASW and MAM recordings were used as input for joint inversion. The resulting  $V_s$  profiles from inversion using different layer models are well representative of the experimental data at the presented sites. The joint inversion was not constrained with *a priori* geologic information, yet resulted in reasonable  $V_s$  profiles compared to nearby subsurface stratigraphy. This highlights the potential reliability of non-invasive surface wave measurements in Metro Vancouver. Further validation of the non-invasive seismic methods and the inverted layered earth models shall be accomplished at deep sites with invasive  $V_s$  measurements. This inter-method comparison will help in explaining and calibrating characteristics and trends of the experimental data in Metro Vancouver within their physical and geologic context. The current collected surface wave measurements in Vancouver enable estimation of theoretical 1D site response using inverted  $V_s$  profiles at strong motion stations. A comparison between theoretical and observed site response shall provide deeper insights on the seismic hazard in Metro Vancouver.

## ACKNOWLEDGMENTS

Funding support is provided by Emergency Management British Columbia (EMBC) and the Institute for Catastrophic Loss Reduction (ICLR). We thank the following University of Western Ontario graduate students in the field data collection: Sujan Adhikari, Alireza Javanbakhht Samani, Ali Fallah Yeznabad, Meredith Fyfe, Sameer Ladak, Alex Bilson Darko, and Christopher Boucher. We also acknowledge additional data processing accomplished by Meredith Fyfe and Sameer Ladak.

## REFERENCES

1. Adams J, Rogers G, Halchuk S, McCormack ., and Cassidy J. (2002). The case for an advanced national earthquake monitoring system for Canada's cities at risk. 7th U.S. National Conference on Earthquake Engineering.
2. Cassidy JF, Rogers GC (2004) Variation in ground shaking on the Fraser River delta (Greater Vancouver , Canada) from analysis of moderate earthquakes. 13th World Conference on Earthquake Engineering 7.
3. Borchardt RD (1970) Effects of Local Geology on Ground Motion Near San Francisco Bay. Bulletin of the Seismological Society of America 60:29–61.
4. Borchardt RD (1994) Estimates of Site-Dependent Response Spectra for Design (Methodology and Justification). Earthquake Spectra 10:617–653.
5. Hassani, B., & Atkinson, G. M. (2016). Applicability of the Site Fundamental Frequency as a  $V_{S30}$  Proxy for Central and Eastern North America. Bulletin of the Seismological Society of America, 106(2), 653-664. doi: 10.1785/0120150259.
6. David Teague, Brady Cox, Brendon Bradley, and Liam Wotherspoon (2018) Development of Deep Shear Wave Velocity Profiles with Estimates of Uncertainty in the Complex Interbedded Geology of Christchurch, New Zealand. Earthquake Spectra: May 2018, Vol. 34, No. 2, pp. 639-672.
7. Garofalo, F., Foti, S., Hollender, F., Bard, P. Y., Cornou, C., Cox, B. R., Dechamp, A., Ohrnberger, M., Perron, V., Sicilia, D., and Teague, D., 2016. InterPACIFIC project: Comparison of invasive and non-invasive methods for seismic site characterization. Part II: Inter-comparison between surface-wave and borehole methods, Soil Dynamics and Earthquake Engineering 82, 241–254.
8. Hunter, J.A. and Atukorala, U. (2015). Chapter 1.0: Introduction; in Shear Wave Velocity Measurement Guidelines for Canadian Seismic Site Characterization in Soil and Rock, (ed.) J.A. Hunter and H.L. Crow; Geological Survey of Canada, Open File 7078, 8-17.
9. Foti, S., Lai, C., Rix, G., and Strobbia, C., 2014. Surface Wave Methods for Near-Surface Characterization, CRC Press.
10. Foti, S., Hollender, F., Garofalo, F., Albarello, D., Asten, M., Bard, P-Y., Comina, C., Cornou, C., Cox, B., Di Giulio, G., Forbriger, T., Hayashi, K., Lunedei, E., Martin, A., Mercerat, D., Ohrnberger, M., Poggi, V., Renalier, F., Sicilia, D., and Socco, V., 2017. Guidelines for the good practice of surface wave analysis: A product of the InterPACIFIC project, Bulletin of Earthquake Engineering, 1–54, doi:10.1007/s10518-017-0206-7.
11. Clague J. (1998) Geology and Natural Hazards of the Fraser River Delta, British Columbia. In: Clague JJ, Luternauer JL, Mosher and DC (eds) Bulletin 525. Geological Survey of Canada, pp 7–16.
12. Britton JR, Harris JB, Hunter JA, Luternauer JL (1995) The bedrock surface beneath the Fraser River delta in British Columbia based on seismic measurements. In: Current Research 1995-E. Geological Survey of Canada, pp 83–89
13. Hunter JA, Christian HA (2001) Use of Shear Wave Velocities to Estimate Thick Soil Amplification Effects in the Fraser River Delta, British Columbia. Symposium on the Application of Geophysics to Engineering and Environmental Problems 2001 SS11-SS11. <https://doi.org/10.4133/1.2922943>.
14. Hunter JA, Burns RA, Good RL, Pelletier C. (2016) Fraser River Delta – A compilation of shear wave velocities and borehole geophysics logs in unconsolidated sediments of the Fraser River Delta, British Columbia. Geological Survey of Canada Open File:1–112.
15. Taylor GW, Monahan P, White TW, Ventura CE (2006) British Columbia school seismic mitigation program: Dominant influence of soil type on life safety of Greater Vancouver and Lower Mainland schools of British Columbia. In: 8th U. S. National Conference on Earthquake Engineering, San Francisco, California
16. Kaya Y, Ventura C (2015) British Columbia Smart Infrastructure Monitoring System (BCSIMS). Proc IWSHM 2015 588:579–588. <https://doi.org/10.1139/cjce-2016-0577>.
17. Wathelet M (2008) An improved neighborhood algorithm: Parameter conditions and dynamic scaling. Geophysical Research Letters 35:L09301. <https://doi.org/10.1029/2008GL033256>.
18. Konno K, Omachi T (1998) Ground-motion characteristics estimated from spectral ratio between horizontal and vertical components of microtremor. Bulletin of the Seismological Society of America 88:228–241.
19. Bettig B, Bard PY, Scherbaum F, et al (2004) Practical experience using simplified procedure to measure average shear-wave velocity to a depth of 30 meters ( $V_{S30}$ ). In: 13th World Conference on Earthquake Engineering.
20. Lacoss RT, Kelly EJ, Toksöz MN (1969) Estimation of seismic noise structure using arrays. Geophysics 29:21–38.
21. Martin, A. J., and J. G. Diehl (2004). Practical experience using a simplified procedure to measure average shear-wave velocity to a depth of 30 meters ( $V_{S30}$ ). in Proceedings, 13th World Conference on Earthquake Engineering, Vancouver, B.C., Canada, August 2004.
22. Onur T, Molnar S, Cassidy J, et al (2004) Estimating site periods in Vancouver and Victoria, British Columbia using microtremor measurements and SHAKE analyses. Canadian Geotechnical Conference, Quebec City, Quebec 24–27.
23. Armstrong JE (1984) Environmental and Engineering Applications of the Surficial Geology of the Fraser Lowland, British Columbia.